Sol-Gel derived thick coatings and their thermomechanical and optical properties

M. Mennig, G. Jonschker, H. Schmidt

Institut für Neue Materialien GmbH, 6600 Saarbrücken, Germany

ABSTRACT

The preparation of crackfree and transparent SiO_2 coatings on soda lime glass with thicknesses of about 8 μm after densification at 500 °C is presented. The high thickness can be obtained by using an 80:20 mixture of methyltriethoxysilane and tetraethyl orthosilicate as alkoxide precursors in combination with an aqueous colloidal SiO_2 sol with particle sizes of about 7 nm. This principle of synthesis is also applied to ZrO_2 containing coatings yielding to thicknesses of about 3 μm. Refractive index measurements indicate that the coatings are nearly completely densified. At higher temperatures tensile stresses appear within the layers and are transmitted to the substrate, increasing its thermal stability.

1. INTRODUCTION

Since the possibility of depositing oxide coatings via the sol-gel process was discovered in 1939[1], one main aim was to increase the thickness of these layers. This problem involves the synthesis of the coating solution, the homogeneous deposition of the liquid film, the drying process and the final densification. The cracking of films usually occurs when the solvents are removed from the gelled film. This is due to capillary forces when the liquid/gaseous interface of the evaporating solvent moves into the gel structure. Another source for the generation of cracks is the mismatch of the coefficients of thermal expansion between the substrate and the film. In a review on sol-gel technologies by Brinker and Scherer[2] it is concluded from the experimental results of the last 30 years that the upper thickness limit obtained by a single step dip coating process is 1 μm. Further increase should only be possible by multiple coating processes. Lange[3] applied the Griffith criterion for crack extension (a crack will increase its length whenever it can lower the free energy of the system) to a drying gel film on a hard substrate and found, that for films thicker than a critical thickness t_c cracking is most probable if small cracks or flaws preexist within the film. t_c is given by equation (1):

$$t_c = E\,G_c / (A\,\sigma^2) \qquad (1),$$

where E is the elastic modulus of the film, σ represents a biaxial tensile stress that arises because the film shrinkage is constrained by the substrate and G_c is the energy required to form two new crack surfaces per unit area. Because A represents a material dependent, combined, dimensionless proportionality constant it is quite difficult to use eq. (1) for a quantitative analysis. But qualitatively one may conclude from eq. (1) that the main contribution to crack formation comes from the stress σ which is a result of the strong interaction of the sol particles or macromolecules, combined with high shrinkage rates. Gels with a more flexible structure should allow stress relaxation processes (lower σ^2 in eq. (1)) and higher critical thicknesses.

Therefore, our approach to thicker SiO_2 coatings was to increase first the flexibility of the gel by decreasing the particle interaction in the sol and in the gel by increasing the solid content.

0-8194-0931-6/92/$4.00

2. EXPERIMENTAL

2.1. Synthesis

To obtain pure SiO_2 and ZrO_2 doped SiO_2 coatings methyltriethoxysilane (MTEOS), tetraethyl orthosilicate (TEOS), zirconium(IV) butoxide ($Zr(-OBu)_4$) 80 % solution in n-Butanol and zirconium(IV) propoxide ($Zr(n\text{-}OPr)_4$ 70 % solution in n-propanol were used as sol precursors. BAYER Kieselsol (type 300) with an SiO_2 content of 30 weight-% and an average particle size of about 7 nm was used as a colloidal dispersion of silica. Sols with different compositions (sol A - E) were synthesized in the following way:

For sol A, a pure SiO_2 sol without colloids, 100 mmole MTEOS, 27 mmole TEOS and 23 mmole ethanol were stirred and a mixture of 330 mmole H_2O, 2.64 mmole HCl_c and 23 mmole ethanol was added. In order to synthesize a colloid containing SiO_2 sol (sol B) 100 mmole MTEOS and 27 mmole TEOS were stirred vigorously using a rotor/stator dispersor and 43 mmole SiO_2 as colloidal dispersed particles were added and after 10 seconds the pH of the solution was adjusted at 1-2 by 2.37 mmole HCl_c. The oxide content of the commercial colloidal silica sol was increased by a rotary evaporator up to 55 weight-% achieving a sol with a final oxide content up to 500 g/l that was stable for 4 hours.

In the sols C - E ZrO_2 was introduced additionally in order to change the refractive index of the appropriate coatings. In sol C molecularly dispersed Zr was introduced into a colloid-free MTEOS/TEOS system synthesized by stirring 96 mmole MTEOS and 17 mmole TEOS and adding a mixture of 55 mmole H_2O, 23 mmole ethanol and 0.66 mmole HCl_c. 5.63 mmole $Zr(n\text{-}OBu)_4$ (80 % solution in n-Butanol) and 23 mmole ethanol were mixed and given to the prehydrolized alkoxides under vigorous stirring after 5 minutes. One minute later 228 mmole H_2O and 30 mmole ethanol were added to complete the hydrolysis.

For sol D ZrO_2 colloids were used instead of SiO_2 colloids. Therefore, a clear water based ZrO_2 sol with a mean particle diameter of 4 nm (measured by dynamic laser light scattering) was prepared as described in [4] by HNO_3 hydrolysis of $Zr(n\text{-}OPr)_4$. The solid content of this sol was 5 weight-% ZrO_2. For the preparation of the silicon alkoxides, 100 mmole MTEOS and 27 mmole TEOS were vigorously stirred using a rotor stator disperser and was added to 0.6 mmole colloidal ZrO_2.

In sol E Zr again was introduced in a molecularly dispersed way but into a SiO_2 colloid containing system. Therefore, sols B and C were slowly mixed under continous stirring immediately after their preparation. Each sol was filtered 30 minutes after preparation using a disposable 0.8 μm filter.

Microscopy slides as well as float glass plates and fibres were used as dip coating substrates. The coating apparatus was installed in a glove box, standing in a clean room (class 10,000). The air humidity was adjusted at 15 $\pm$ 5 rel.%. To control the coating thickness the withdrawal speed was varied from 0.5 to 10.5 mm/s. The samples were dried for 15 minutes at 60 °C under clean room conditions and then heated from room temperature to 400 °C with a rate of 1 K/min and from 400 to 500 °C with 0.3 K/min. This temperature was held for 15 minutes and then the samples were cooled down to room temperature within 10 h.

2.2. Characterisation

The thickness of the coatings was measured with a profilometer with diamond stylus at a step, made by scratching the coating with a plastic knife after drying at 60 °C.

The refractive index of a coating was determined from a VIS transmission spectrum of a microscopic slide coated on both sides, with an uncoated slide as reference. Such spectra show sine curves with minima at about 100 % transmission if the refractive index of the coating is lower than the refractive index of the substrate. Otherwise the maxima of the sine curve are at about 100 % transmission. These

minima and maxima origin from an interference effect. One can calculate the refractive index of the coating n_c for wavelengths λ_m, where the thickness of the coating is an odd multiple member of $\lambda/4$ using [5]

$$n_c = n_s \cdot \frac{1 + R^{1/2}}{1 - R^{1/2}}^{1/2} \quad \text{where} \tag{2}$$

the reflectance R is

$$R = \frac{(1 + R_o) - (1 - R_o)\, T_m}{(1 + R_o) + (1 - R_o)\, T_m} \tag{3}$$

T_m in eq. (3) is the measured transmittance at an interference extremum (for high refractive coatings at a maximum) at wavelength λ_m. R_o is the reflectance of the uncoated substrate and can be calculated from the Fresnel formula, see eq. (4)

$$R_o = \frac{(1 - n_s)^2}{(1 + n_s)^2} \tag{4}$$

where n_s is the refractive index of the substrate. The thickness of the caoting d_c can be obtained from

$$d_c = m \cdot \frac{\lambda_m}{4\, n_c} \tag{5}$$

where n_c is the refractive index determined with formula (2) and m is the order of the extremum and can be calculated with

$$m = \frac{\lambda_m}{\lambda_m - \lambda_o} \tag{6}$$

where λ_o is the wavelength of the extremum next to λ_m with $\lambda_o < \lambda_m$. The refractive index of the substrate n_s was measured with a Pulfrich refractometer for visible light as a function of wavelength.

In order to investigate the thermomechanical behaviour of coated soda lime glass at high temperatures a fibre elongation viscosimeter experiment was carried out with dip coated and uncoated fibres of about 50 mm in length and 0.8 mm in diameter that had been drawn from 4 mm thick soda-lime glass rods.

For a crash test coated and uncoated microscopic slides were heated with a solder burner up to 1750°C and time was measured until the slides were melted and dropped down. In addition to this, float glass plates of 4 mm thickness were coated with the sols A, B and C and then cut into stripes of 2 x 10 cm^2. The stripes were mounted in a steel frame and kept for 4:30 minutes at 850°C in a furnace.

3. RESULTS AND DISCUSSION

3.1. Sol synthesis

In order to develop systems with reduced particle interaction and increased solid content a new concept had to be realized. For an increased solid content, silica dispersed in an aqueous solution and stabilized with NaOH was chosen as precursor. To combine the aqueous colloidal silica with tetraethyl orthosilicate (TEOS) and methyltriethoxysilane (MTEOS), some difficulties had to be overcome. The aqueous sol is stabilized at pH 8 - 9 and reacts very sensitive to pH changes or dilution with alkohols. At low pH values, rapid gelation occurs. For sufficient hydrolysis rates of the MTEOS/TEOS system, however, low pH values are necessary. It was found that the aqueous system and the MTEOS/TEOS system are immiscible as long as hydrolysis is avoided. By heavy stirring, emulsions can be prepared mechanically. Contrary to our expectations addition of HCl to the emulsion does not lead to precipitates but to clear solutions with particle sizes of about 8 nm in diameter according to PCS measurements. Since the emulsion is completely non-transparent, the droplet size is estimated to be in the range of 0.2 to 0.5 μm at least. So far the precipitates are expected to be in the same range. The fact that HCl in the emulsion does not activate the coagulation of the SiO_2 particles as it does in the pure sol, has to be explained by some interaction of hydrolysed species of the MTEOS/TEOS system, preventing the particle interaction by condensation of surface ≡Si-OH groups (see fig. 1).

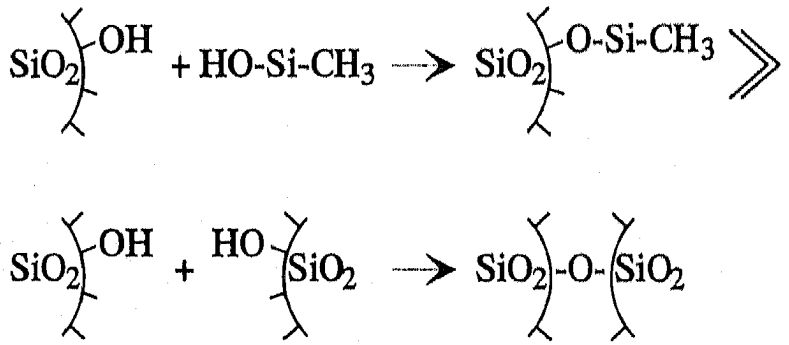

Fig. 1: Inhibition of condensation of SiO_2 nanoparticles by surface covering

It is assumed that the surface covering of the sol particles by HO-Si-CH_3 or HO-Si-OCH_3 is the faster reaction compared with the condensation of two nanoparticles as schematically shown in fig. 1.

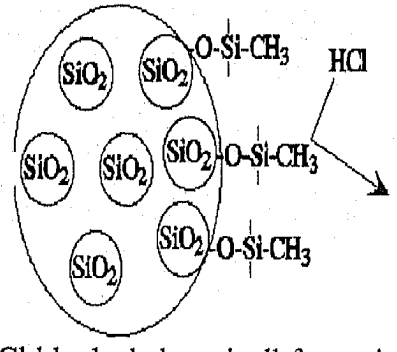

Fig. 2: HCl blockade by micell formation

This can be explained by higher diffusion rates of monomolecular species compared to the particles. Another explanation might be the formation of micelles by interface interaction of partially hydrolysed species reducing the diffusion rate of the HCl into the droplet as pointed out in fig. 2. After the hydrolysis of the MTEOS/TEOS has reached a sufficient level, the produced ethanol leads to a homogeneous system and the surface coverage of the SiO_2 colloids by MTEOS can take

place. The hypothesis of hydrophobic surface covering is supported by the fact, that these systems lead to substantially higher thicknesses than pure MTEOS/TEOS systems and will be discussed in detail later. The route is schematically shown in fig. 3.

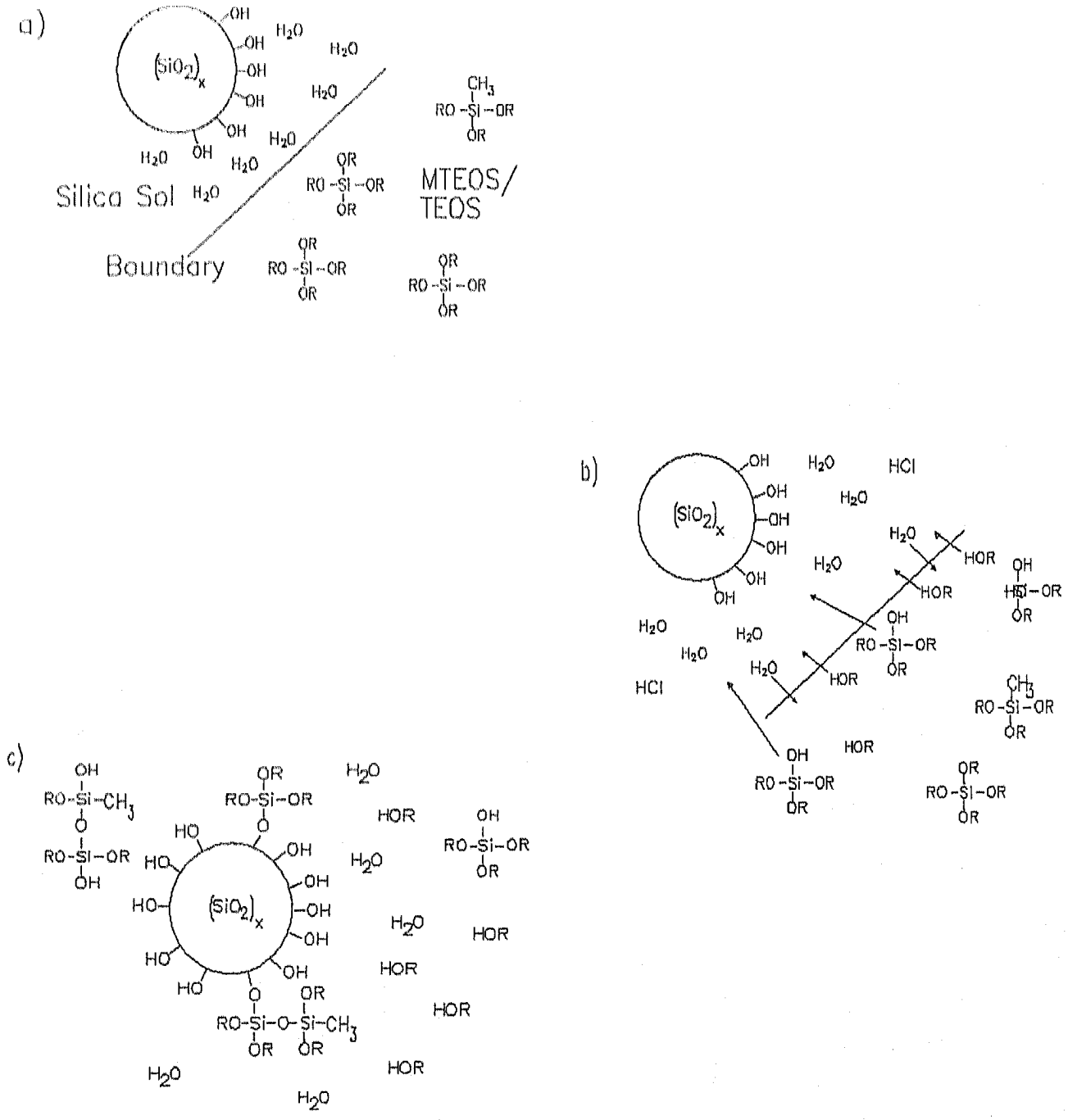

Fig. 3: Synthesis of a coating sol by combination of colloidal silica with alkoxides.

3.2. Fabrication of coatings

In fig. 4 the maximal thickness of crackfree coatings after thermal treatment at 500°C is shown for the different sols. It is obvious that the 'limit' of 1 μm is widely exceeded in each case.

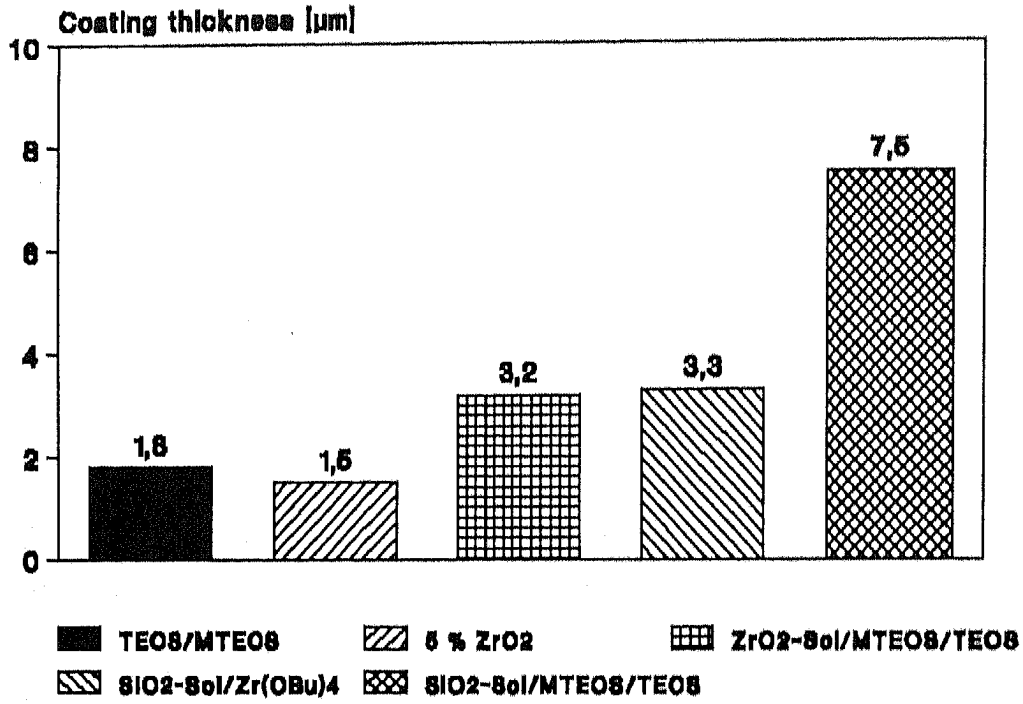

Fig. 4: Maximal coating thickness, obtained after densification at 500 °C

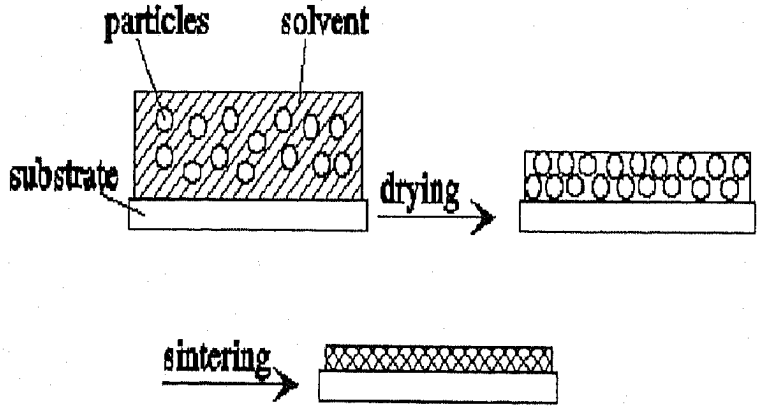

Fig. 5: Schematics of the layer with controlled particle interaction

We assume, that MTEOS suppresses the three-dimensional crosslinking by formation of a $-CH_3$ surface covering. During drying, the low interaction between the particles leads to an enhanced relaxation, as indicated in fig. 5. DTA/TG measurements indicate, that the final crosslinking of the dried gel takes place when the methyl groups are oxidized at temperatures between 400°C and 500°C. Additionally it can be assumed that the unpolar methyl groups provide a hydrophobic effect, thus reducing the capillary forces during drying. The molar ratio of 80 % MTEOS to 20 % TEOS yielded the maximum thickness in this system and was used as a basis for further investigations. The results show that the use of colloidal silica as a "filler" could increase the thickness significantly, but this cannot be explained with the common effect of fillers in the μm range, which increase the pore size and thus lead to improved drying behaviour. Nanoscaled particles with diameters of only 7 nm are not able to increase the pore radii substantially. Reduction of interaction and increased solid content lead to lower tensile stresses and this is very evident for the increase of the "critical thickness" as predicted by Lange's equation (1).

For ZrO_2 containing sols with $Zr(n\text{-}OBu)_4$ as precursors, the maximum thickness decreased with increasing ZrO_2 from 1.6 μm for 5 % to 1.0 μm for 20 % ZrO_2. As already observed with SiO_2 the addition of colloidal ZrO_2 allows to prepare much more thicker (3.2 μm) coatings too. The effect of the nm sized "filler" is assumed to be similar to that for the colloidal silica. We assume further that the surface modification effect will be lower than in the case of the silica sol, beause the ZrO_2 sol consists of condensed $ZrO(NO_3)(OH)$ species not able to react with ≡Si-OH groups. For the mixture of the sol with colloidal silica (sol B) and the ZrO_2 sol obtained after the prehydrolysis (sol C) the possible coating thickness was nearly the same as for that with colloidal ZrO_2. This can also be explained with the low filler content in this sol, because the silica sol was 'diluted' with the SiO_2/ZrO_2 sol.

3.3. Optical properties

Fig. 6 shows the dispersion of a pure SiO_2 coating after densification at 400 °C and at 500 °C calculated with the formulas (2) - (4). As expected the refractive index is decreasing with increasing wavelength and is higher at 500 °C (n_D = 1.452) than at 400 °C (n_D = 1.446). The accuracy of the applied method for the determination of the refractive index in the wavelength region between 550 and 600 nm can be estimated from this figure to be about $\Delta n = \pm 0.003$. A comparison between the values of the thickness d of the coatings, measured by profilometer (d = 5.7 μm for 400 °C and d = 5.0 μm for 500 °C) and the average thicknesses d_c calculated with equation (4) using the independently calculated values n_c (d_c = 5.65 ± 0.24 μm for 400 °C and d_c = 5.12 ± 0.18 μm for 500 °C) shows very good agreement. This demonstrates the usefulness of this method for the determination of the thickness as well as for the refractive index.

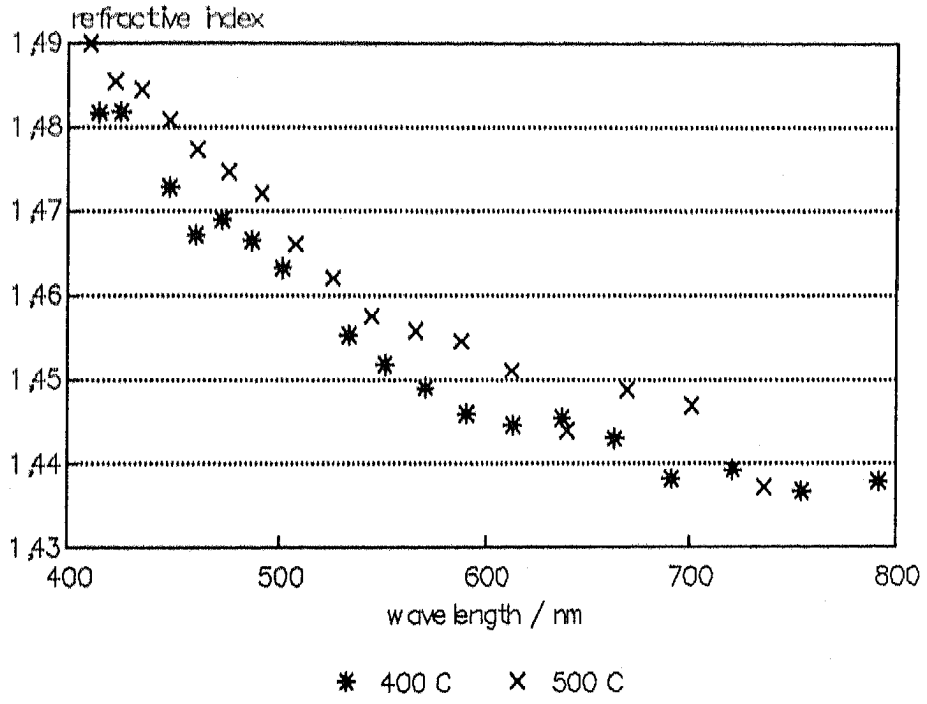

Fig. 6: Dispersion of a SiO_2 coating after densification at 400 °C and 500 °C.

As expected the refractive index of the SiO_2 layer, densified at 500 °C is less than that of fused silica ($n_D \approx 1.460$). This indicates that the layer is not completely densified. From the Lorentz-Lorenz relation[6]

$$\frac{n^2 - 1}{n^2 + 2} \cdot \frac{M}{R} = \rho \qquad (7)$$

the degree of densification can be estimated using the calculated value for n_D (1.452) as refractive index n in eq. (7). Assuming that during densification the molar weight M and the molar refraction R of the SiO_2 layer remain constant one may conclude that the density ρ of the layer densified at 400 °C is about 97 % and at 500 °C is about 98 % of the density of fused silca (n_D = 1.460). With respect to the high transformation temperature T_g of fused silica this represents a surprisingly high level of densification. Impurities from the sol synthesis route can be excluded, but diffusion of Na^+ ions into the SiO_2 layer from the glass substrate cannot be completely excluded. This has to be examined in future.

Table 1 compares the refractive index for pure SiO_2 and ZrO_2 doped layers synthesized with the different sols (A - E).

Table 1:
Refractive index of SiO_2 and SiO_2/ZrO_2 coatings after densification at 400 °C and 500 °C

type		ZrO_2/ mole-%	n_D 400 °C	n_D 500 °C
A:	MTEOS/TEOS	-	1.421 ± 0.005	1.440 ± 0.005
B:	MTEOS/TEOS + colloidal SiO_2	-	1.446 ± 0.0025	1.452 ± 0.0025
C:	MTEOS/TEOS/$Zr(O\text{-}Bu)_4$	2.3	1.406 ± 0.005	1.455 ± 0.005
D:	MTEOS/TEOS + colloidal ZrO_2	2.3	1.430 ± 0.005	1.459 ± 0.005
E:	MTEOS/TEOS/$Zr(O\text{-}Bu)_4$ + colloidal SiO_2	2.3	1.445 ± 0.005	1.461 ± 0.005

Table 1 shows that for all compositions the refractive index increases with increased temperature from 400 °C to 500 °C. Comparing sol A and B one can see, that the introduction of the SiO_2 particles into the sol synthesis yields in denser layers, since the refractive index of this layer is remarkabl higher. Despite their ZrO_2 content type C, D and E show relatively low n_D values at 400 °C compared to B, but they are still higher than A. A possible explanation could be the assumption of a "rigid" network built up by strongly interacting ZrO_2 units and thus preventing densification. At 500 °C all three systems result in higher n_D values. The effect of using colloids can be seen in SiO_2 and ZrO_2 systems. By heating from 400 °C up to 500 °C n_D is remarkably increased in non-colloidal systems, indicating different densification mechanisms. So it can be concluded that colloidal systems lead to thicker and denser layers than non-colloidal ones.

3.4. Thermomechanical properties

the estimated densities of 97 to 98 % of the theoretical density of fused silica suggests T_g values close to 1000 °C which is much higher than the T_g of soda lime glass. So the question arises what high temperature properties can be expected from a sandwich system consisting of a soda lime glass plate coated on both sides with a thick SiO_2 coating. A preliminary test was carried out heating up an uncoated and a coated microscopic slide with a solder burner. The uncoated slides were melted and

dropped down after 55 seconds, whereas the slides coated with SiO_2 became 'unmeltable' remained in a nearly rectangular shape when the coating thickness exceeded 2 μm. Similar results were obtained by using 4 mm thick plate glass.

These tests very well demonstrate the thermal protection effect of the coatings on soda lime glass. For investigating the phenomena in more detail a fibre elongation experiment was carried out with a SiO_2 coating on a soda lime glass fiber. Fig. 7 shows the results of this measurement.

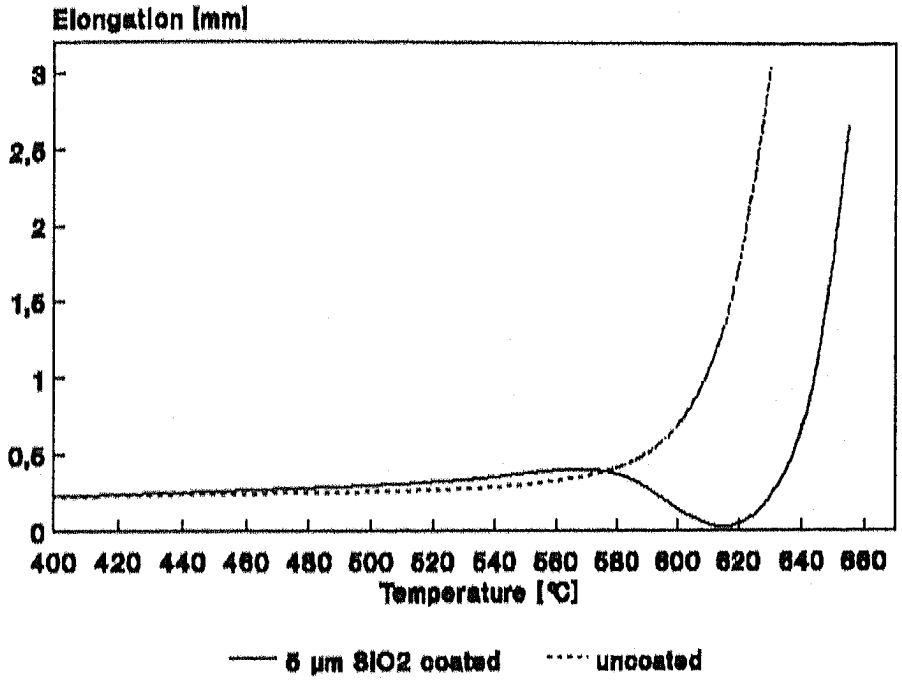

Fig. 7: Fiber elongation viscosimetry of a 5 μm SiO_2 coated fibre compared to an uncoated fiber under the load of 20 g.

The uncoated fiber shows the expected behaviour. For temperatures higher than 540 °C it starts elongating under the influence of the 20 gramm weight. In opposition to this, the 5 μm thick SiO_2 coating is able to lift this weight nearly 0.5 mm at a temperature when the substrate glass is softening. At this time the fiber is even shorter than at the beginning of the experiment, that means the coating causes a shrinkage effect against the 20 gramm weight. The obtained contraction of the coated fibre of about 0.5 mm at a total length of about 50 mm corresponds to a volume shrinkage of about 3 %. This very roughly estimated value is in good agreement with the result of the refractive index measurement that indicated a degree of densification of about 97 %. As one can see from fig. 7 the densification of the SiO_2 layer takes place at far lower temperatures than the T_g of fused silica. This seems to be a question of the SiO_2 structure in this layer. This result proves, that the shrinking coating is able to transfer mechanical forces to the substrate. Crystallization effects could also be the reason for this shrinkage, but this has to be checked in further experiments.

From the thermomechanical investigations the conclusion can be drawn that the thermal protection of the coating on slides and plate glass results from two effects. For temperatures near the T_g of the substrate up to about 620 °C the shrinkage of the coating causes tensile stresses that prevent the substrate from deformation. At higher temperatures the coating is densified and forms a high T_g layer stable enough to avoid remarkable softening of the sandwich.

4. CONCLUSIONS

The experiments with nm sized surface modified colloidal silica sols have shown, that it is possible to obtain much more thicker sol-gel coatings than usually. As a consequence of this experimental findings it has to be concluded that considerations for critical thickness of sol-gel coatings have to take into

account the type and intensity of interactions between the gel particles, since tthis effects strongly stress relaxation in the drying gel. So the thesis of an upper limit for the thickness of a sol-gel layer has to be interpreted in a more complex way. The investigated colloidal SiO_2 system shows a relatively high degree of densification at temperatures substantially lower than T_g of the appropriate melted glass. This very interesting effect has to be investigated in future in order to be able to relate it to structural phenomena. Furthermore, thick sol-gel coatings on glass open up some very interesting possibilities for applications in the field of planar waveguides or for thermal protection purposes of flat glass.

5. LITERATURE

1. W. Geffcken, E. Berger, Dtsch. Reichspatent 736411 (1939) Jenaer Glaswerk Schott u. Gen. Jena
2. C.J. Brinker, G.W. Scherer, "Sol Gel science-The physics and chemistry of Sol Gel Processing", Academic Press Inc. 1990
3. F. Lange, "Liquid Precursors for Ceramic Particles, Fibers and Thin Films", Proceedings of the International Symposium on Molecular Level Designing of Ceramics, p. 14-28, March 16 1991 Nagoya, Japan.
4. G. Rinn, H. Schmidt, "Preparation of Y-doped zirconia by emulsion technique", Proceedings of the second international conference on ceramic powder processing science, p. 221-228, Berchtesgaden oct. 12-14 1988,
5. F. Abelés, "Methods for determining optical parameters of thin films", Progression in Optics, volume II, p. 249 - 288, Elsevier Amsterdam - Oxford - New York - Tokyo, 1963
6. D'Ans, Lax (ed. M. D. Lechner), "Magnetische, elektrische und optische Konstanten", Taschenbuch für Chemiker und Physiker 1, p. 503, Springer Verlag Berlin, Heidelberg, New York, London, Paris, Tokyo, Hong Kong, Barcelona, Budapest